

Enhanced photocatalytic water oxidation on ZnO photoanodes in a borate buffer electrolyte

Cite this: *Catal. Sci. Technol.*, 2013, **3**, 1699Received 28th January 2013,
Accepted 8th March 2013

DOI: 10.1039/c3cy00062a

www.rsc.org/catalysisFeng-Qiang Xiong,^{ab} Jingying Shi,^a Donge Wang,^a Jian Zhu,^a Wen-Hua Zhang^a and Can Li^{*a}

Water oxidation performance of ZnO photoanodes was improved with a negative shift of ~0.2 V in potential by a simple *in situ* photoelectrochemical reaction in borate buffer solution (B_{BS}) or immersion at 75 °C in concentrated B_{BS}. Electrochemical study of FTO electrodes shows an overpotential reduction effect of B_{BS} treatment.

Solar fuels can be produced from photocatalytic, photoelectrochemical or photovoltaic–electrochemical splitting of H₂O and conversion of CO₂. In these processes, the water oxidation reaction is involved. The water oxidation reaction is complicated with transfer of 4 electrons and 4 protons. Calculation results showed that the free energy change of the rate-controlling step of water oxidation is as high as ~0.6 eV at the overpotential of 0.7 V on the TiO₂ surface,¹ and transient absorption spectroscopy revealed that the water oxidation is as slow as on the scale of sub-seconds.² On the other hand, the valence bands of semiconductors like TiO₂ are still sufficiently positive to meet the energy requirement. As an analogue of TiO₂, ZnO is similar in band gap and positions of CB and VB.³ ZnO has been studied as a photoanode for water oxidation as well,^{4–6} but gives insufficient efficiency. There are some other reasons for low efficiency of water oxidation on photoanodes. Most photo-generated holes are trapped by defect sites or surface species except for intrinsic recombination.^{2,7,8} The trapping reduces the energy of holes and thus the oxidizing ability. Furthermore the trapped sites and surface species may act as recombination centers which results in a much shorter lifetime of the holes. Most holes are recombined before driving water oxidation reaction, so the quantum efficiency (QE) is very low. Applying high potential on the photoanode inhibits recombination by extracting electrons, but it requires external bias and thus consumes external energy.⁹

In order to increase the QE, one way is to remove the recombination centers by improving the crystallinity of the semiconductor and by surface modification.^{10,11} Another way is to change the path of water oxidation to lower the kinetic barrier and reduce the overpotential required for water oxidation.

Cocatalysts are deposited on the semiconductor photoanode to reduce the overpotential of water oxidation reaction, such as IrO₂,^{12,13} Co₃O₄,^{13–15} FeOOH,¹⁶ and a Co-based catalyst deposited with phosphate buffer (known as Co–Pi).^{6,17–19} In the studies using Co–Pi as a cocatalyst, usually phosphate buffer solution is also employed as an electrolyte, following the original research on electrocatalytic water oxidation using Co-based catalysts deposited with various buffers including phosphate, methylphosphate and borate.^{20,21} A few studies showed that the activity of the assisted photoanodes in a buffered phosphate electrolyte is higher than that in an unbuffered sulfate electrolyte with the same pH.²² In this work, we found that even without adding a source of valence-variable metals, such as Fe, Co or Ni, water oxidation on ZnO photoanodes was enhanced by *in situ* photoelectrochemical reaction in B_{BS} or treatment at 75 °C in concentrated B_{BS}.

ZnO photoanodes used in this study were fabricated on FTO with a seed layer by galvanostatic cathodic deposition from a solution of 5 mM Zn(NO₃)₂ and 50 mM KNO₃ at 70 °C. A base forms from the reduction of NO₃[–] and precipitates the Zn²⁺ as ZnO.⁶ The resulting electrodes contain the ZnO nanorod (NR) array on FTO, with an average nanorod diameter and length of 39 nm and 230 nm, respectively (Fig. 1). As a result of using the ZnO seed layer, the nanorods are smaller but denser than those prepared by Ellen M. P. Steinmiller *et al.*⁶ Then a post-calcination at 500 °C was employed to improve the crystallinity of ZnO nanorods.

ZnO nanorod (NR) arrays were used as photoanodes and the photocatalytic water oxidation performance in 0.24 mol kg^{–1} B_{BS} (pH 9.3) was tested. After *in situ* photoelectrochemical reaction at 1.43 V (vs. RHE) for 1.5 h with 0.24 mol kg^{–1} B_{BS} as the electrolyte, the photocurrent–potential characteristic of the ZnO electrode was improved remarkably with a decrease of ~0.2 V in potential (Fig. 2a), and the photocurrent for water

^a State Key Laboratory of Catalysis, Dalian Institute of Chemical Physics, Chinese Academy of Sciences and Dalian National Laboratory for Clean Energy, Dalian 116023, China. E-mail: canli@dicp.ac.cn; Web: <http://www.canli.dicp.ac.cn>; Fax: +86 411 84694447; Tel: +86 411 84379070

^b Graduate University of Chinese Academy of Sciences, Beijing 100049, China

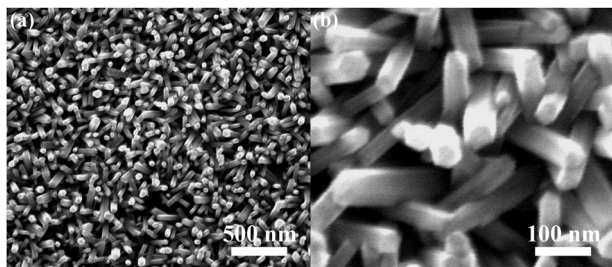


Fig. 1 SEM images of ZnO NR array from cathodic deposition onto ZnO seeded FTO with current density of 0.05 mA cm^{-2} for 5000 s in 5 mM $\text{Zn}(\text{NO}_3)_2$ and 50 mM KNO_3 . (b) An enlarged part of (a).

oxidation at 0.73 V (vs. RHE) was enhanced 6.5 fold (Fig. 2b). The photoanode after photoelectrolysis kept the ZnO phase, as characterized by XRD (Fig. 3). In the other case, ZnO photoanodes were treated by immersion in various concentrations of B_{BS} at 75°C for 1.5 hours. In Fig. 4a, it is shown that ZnO electrodes after immersion in 1 mol kg^{-1} and 2 mol kg^{-1} B_{BS} performed better with a negative shift of $\sim 0.1\text{--}0.2 \text{ V}$ in potential compared to the untreated sample, respectively. After immersion in 4 mol kg^{-1} B_{BS} , the photocurrent at a potential lower than 1 V (vs. RHE) was enhanced more than that of those treated with low concentrations of B_{BS} , while the photocurrent at a potential higher than 1.5 V (vs. RHE) was decreased. The decrease in photocurrent with reduction in overpotential resulted from the reaction of partial ZnO with highly concentrated B_{BS} during immersion, as ZnO was found to be dissolved after immersion in 4 mol kg^{-1} B_{BS} for 29 hours. As Fig. 4b

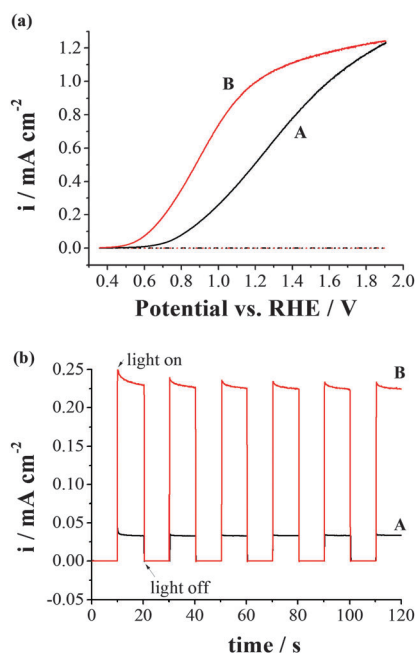


Fig. 2 Photocurrent–potential characteristics (positive scan, scan rate, 10 mV s^{-1}), and (b) photocurrents (measured at 0.73 V vs. RHE with chopped light) of ZnO NR arrays before (A, black solid) and after (B, red solid) *in situ* photoelectrolysis at 1.43 V vs. RHE for 1.5 hours in 0.24 mol kg^{-1} B_{BS} (pH 9.3). The dot lines in (a) which seem overlapped show the dark currents.

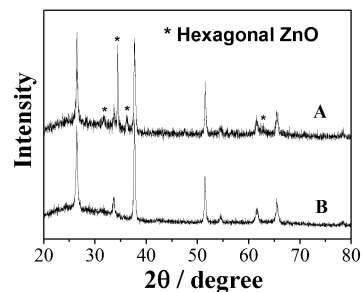


Fig. 3 XRD patterns of (A) photoanode after *in situ* photoelectrolysis at 1.43 V vs. RHE for 1.5 hours in 0.24 mol kg^{-1} B_{BS} (pH 9.3) and (B) the FTO substrate.

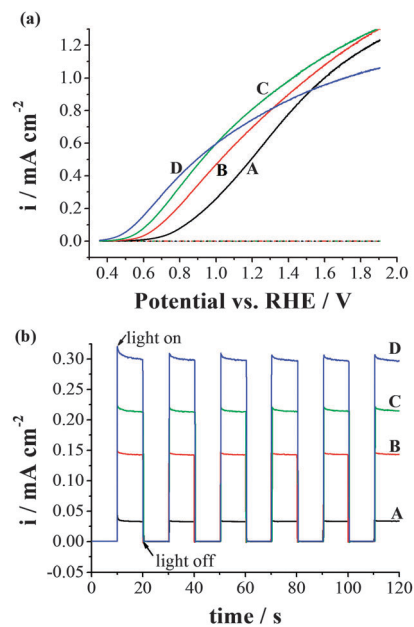


Fig. 4 (a) Photocurrent–potential characteristics (positive scan, scan rate, 10 mV s^{-1}), and (b) photocurrents (measured at 0.73 V vs. RHE with chopped light) in 0.24 mol kg^{-1} B_{BS} (pH 9.3), of ZnO electrode (A, black solid) and ZnO electrodes after immersion in 1 mol kg^{-1} (B, red solid), 2 mol kg^{-1} (C, green solid) and 4 mol kg^{-1} (D, blue solid) B_{BS} at 75°C for 1.5 hours, respectively. The dot lines in (a) which seem overlapped show the dark currents.

shows, the photocurrents at 0.73 V (vs. RHE) of treated ZnO were 4, 6 and 9 fold of that of the untreated sample, respectively. Therefore, the activity of photoelectrocatalytic water oxidation is positively related with the concentration of borate employed in the immersion treatment.

To investigate the mechanism of enhancement in water oxidation on the ZnO photoanode, the borate treatment effect on electrochemical water oxidation was studied on FTO electrodes and Al-doped ZnO (AZO) electrodes (a commercial analog of FTO used as a conductive substrate in solar cells). Water oxidation on FTO and AZO electrodes was improved after immersion in 1 mol kg^{-1} B_{BS} at 75°C for 12 h as well (Fig. 5). The overpotential decreased by around 0.12 V and 0.16 V on the FTO electrode and the AZO electrode after borate treatment, respectively.

It is accepted that borate anions in the electrolyte act as proton acceptors sustaining the proton coupled electron transfer

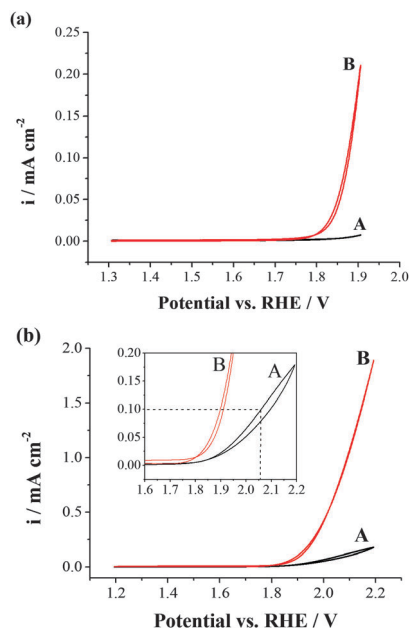
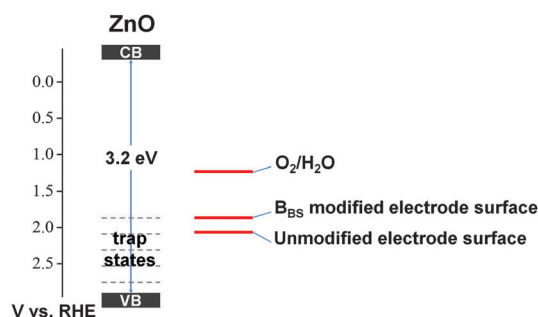


Fig. 5 (a) CV characteristics (scan rate, 50 mV s^{-1}) of an untreated FTO electrode (A, black solid) and a FTO electrode after immersion in $1 \text{ mol kg}^{-1} \text{ B}_{\text{BS}}$ at 75°C for 12 hours (B, red solid). (b) CV characteristics (scan rate, 50 mV s^{-1}) of an untreated FTO electrode (A, black solid) and a FTO electrode after immersion in $1 \text{ mol kg}^{-1} \text{ B}_{\text{BS}}$ at 75°C for 12 hours (B, red solid). Zooming in of the figure gives the inset.

(PCET) route.^{21,23} Moreover, the surface of the ZnO photoelectrode was modified during photoelectrochemical reaction or immersion in B_{BS} . The electrochemical water oxidation result indicates that adsorbed borate species formed on the electrodes contribute to the enhancement of water oxidation by decreasing the overpotential. The coordination effect of borate anions on the surface may lower the energy position of the intermediate of water oxidation. As shown in Scheme 1, the potential of water oxidation on the unmodified ZnO surface is estimated from the potential at a considerable current density of 0.1 mA cm^{-2} on the AZO electrode (2.06 V vs. RHE, shown in the inset of Fig. 5b), and the potential on the B_{BS} modified ZnO surface is about 0.2 V more negative than that on the unmodified ZnO surface. Lower overpotential means a lower kinetic barrier to be overcome for water oxidation reaction, which gives more opportunities for the photogenerated holes to participate in water oxidation reaction.



Scheme 1 Relevant energy levels on ZnO photoanodes.

On the other hand, with the ability to catalyze electron transfer both forward and backward, valence-variable metals or oxides as cocatalysts with even lower water oxidation overpotential probably play the role of recombination or back reaction catalysis centers, which is avoided on the B_{BS} modified photoanode with moderate overpotential resulting from the barrier of bidirectional electron transfer reaction. Both *in situ* photoelectrochemical reaction in B_{BS} and immersion in hot concentrated B_{BS} promote the formation of catalytic species. More work is needed to explore the detailed mechanism including the composition, structure and formation of the catalytic species.

Conclusions

We demonstrated a simple method to improve the photocatalytic water oxidation performance of a photoanode in B_{BS} . During photoelectrolysis or immersion in B_{BS} , the surface of the ZnO photoelectrode was modified. The modification of the ZnO photoanode with borate anions on the surface lowers overpotential and thus enhances the activity of photocatalytic water oxidation.

Experimental section

Preparation of ZnO electrodes

ZnO NR arrays on FTO were fabricated by galvanostatic deposition in a two-electrode cell, a modified version of the potentiostatic deposition described by Ellen M. P. Steinmiller *et al.*⁶ Firstly, a seed layer of ZnO was deposited on FTO glass by spin coating a solution of 0.75 M zinc acetate and 0.75 M monoethanolamine in 2-methoxyethanol and subsequent calcination at 500°C for 30 min. FTO with the ZnO seed layer and Pt were used as the cathode and the anode with a working area of 1.8 cm^2 and 4 cm^2 , respectively. The electrolyte contained $5 \text{ mM Zn}(\text{NO}_3)_2$ and 50 mM KNO_3 . After keeping the electrolyte and electrodes in 70°C bath for about 12 min, electrolysis with a current density of 0.05 mA cm^{-2} on the FTO electrode led to the growth of ZnO NRs on the seed layer. After deposition for 5000 s, the ZnO NR array on FTO was washed with water and dried under nitrogen flow. The resulting ZnO NR array was annealed at 500°C in O_2 for 3 h.

Immersion treatment in concentrated B_{BS}

Concentrated B_{BS} was prepared from $\text{Na}_2\text{B}_4\text{O}_7 \cdot 10\text{H}_2\text{O}$ (analytical reagent) and ultrapure water ($18.2 \text{ M}\Omega \text{ cm}$, PURELAB) without adding any other chemicals, where the concentration of B_{BS} is 4 times that of $\text{Na}_2\text{B}_4\text{O}_7$ in value. A ZnO, FTO or AZO electrode was immersed in sealed 1 mol kg^{-1} , 2 mol kg^{-1} or $4 \text{ mol kg}^{-1} \text{ B}_{\text{BS}}$ at 75°C for hours (*vide supra*), and then was taken out for (photo)electrochemical measurement.

Characterization

SEM images were obtained by using a QUANTA 200FEG scanning electron microscope operated at 20 kV . XRD analysis was carried out using an X-ray diffractometer (Rigaku D/max 2500 PC) using $\text{Cu K}\alpha$ as the radiation source.

(Photo)electrochemical measurement

All electrochemical and photoelectrochemical measurements were carried out in a 3-electrode cell at room temperature, with Pt and a mercurous sulfate electrode as the counter electrode and the reference electrode respectively. The potential measured was converted to RHE by using φ (vs. RHE) = φ (vs. Hg₂SO₄/Hg) + 0.658 + pH 0.0592 (V). 0.24 mol kg⁻¹ B_{BS}, i.e. 0.06 mol kg⁻¹ Na₂B₄O₇ prepared from Na₂B₄O₇ (99.998%, metals basis, Alfa Aesar) and ultrapure water, was used as the electrolyte. Light irradiation from a 140 Xe lamp through a quartz window was used in photoelectrochemical experiments. For photocurrent measurement, the light was chopped for 10 s and passed for another 10 s as a cycle.

Acknowledgements

This work was financially supported by 973 National Basic Research Program of the Ministry of Science and Technology (grant no. 2009CB220010), National Natural Science Foundation of China (grant no. 20873141), Solar Energy Action Plan of Chinese Academy of Sciences (grant no. KGCX2-YW-399+7-3) and the External Cooperation Program of the Chinese Academy of Sciences (grant no. GJHZ1129).

Notes and references

- 1 Y. F. Li, Z. P. Liu, L. L. Liu and W. G. Gao, *J. Am. Chem. Soc.*, 2010, **132**, 13008–13015.
- 2 J. W. Tang, J. R. Durrant and D. R. Klug, *J. Am. Chem. Soc.*, 2008, **130**, 13885–13891.
- 3 Y. Xu and M. A. A. Schoonen, *Am. Mineral.*, 2000, **85**, 543–556.
- 4 A. Wolcott, W. A. Smith, T. R. Kuykendall, Y. P. Zhao and J. Z. Zhang, *Adv. Funct. Mater.*, 2009, **19**, 1849–1856.
- 5 Y. K. Hsu, Y. G. Lin and Y. C. Chen, *Electrochem. Commun.*, 2011, **13**, 1383–1386.
- 6 E. M. P. Steinmiller and K. S. Choi, *Proc. Natl. Acad. Sci. U. S. A.*, 2009, **106**, 20633–20636.
- 7 N. Serpone, D. Lawless, R. Khairutdinov and E. Pelizzetti, *J. Phys. Chem.*, 1995, **99**, 16655–16661.
- 8 Y. Tamaki, A. Furube, M. Murai, K. Hara, R. Katoh and M. Tachiya, *J. Am. Chem. Soc.*, 2006, **128**, 416–417.
- 9 S. R. Pendlebury, M. Barroso, A. J. Cowan, K. Sivula, J. W. Tang, M. Gratzel, D. Klug and J. R. Durrant, *Chem. Commun.*, 2011, **47**, 716–718.
- 10 K. Maeda, H. Terashima, K. Kase, M. Higashi, M. Tabata and K. Domen, *Bull. Chem. Soc. Jpn.*, 2008, **81**, 927–937.
- 11 F. Le Formal, N. Tetreault, M. Cornuz, T. Moehl, M. Gratzel and K. Sivula, *Chem. Sci.*, 2011, **2**, 737–743.
- 12 R. Abe, M. Higashi and K. Domen, *J. Am. Chem. Soc.*, 2010, **132**, 11828–11829.
- 13 Y. Q. Cong, H. S. Park, S. J. Wang, H. X. Dang, F. R. F. Fan, C. B. Mullins and A. J. Bard, *J. Phys. Chem. C*, 2012, **116**, 14541–14550.
- 14 M. J. Liao, J. Y. Feng, W. J. Luo, Z. Q. Wang, J. Y. Zhang, Z. S. Li, T. Yu and Z. G. Zou, *Adv. Funct. Mater.*, 2012, **22**, 3066–3074.
- 15 H. Ye, H. S. Park and A. J. Bard, *J. Phys. Chem. C*, 2011, **115**, 12464–12470.
- 16 J. A. Seabold and K. S. Choi, *J. Am. Chem. Soc.*, 2012, **134**, 2186–2192.
- 17 D. E. Wang, R. G. Li, J. Zhu, J. Y. Shi, J. F. Han, X. Zong and C. Li, *J. Phys. Chem. C*, 2012, **116**, 5082–5089.
- 18 D. K. Zhong, S. Choi and D. R. Gamelin, *J. Am. Chem. Soc.*, 2011, **133**, 18370–18377.
- 19 D. K. Zhong, J. W. Sun, H. Inumaru and D. R. Gamelin, *J. Am. Chem. Soc.*, 2009, **131**, 6086–6087.
- 20 M. W. Kanan and D. G. Nocera, *Science*, 2008, **321**, 1072–1075.
- 21 Y. Surendranath, M. Dinca and D. G. Nocera, *J. Am. Chem. Soc.*, 2009, **131**, 2615–2620.
- 22 M. Higashi, K. Domen and R. Abe, *J. Am. Chem. Soc.*, 2012, **134**, 6968–6971.
- 23 M. Dincă, Y. Surendranath and D. G. Nocera, *Proc. Natl. Acad. Sci. U. S. A.*, 2010, **107**, 10337–10341.